

## **Supporting Information**

### **Optimal size of Fe<sub>3</sub>O<sub>4</sub> nanoparticles for different crops depends on the unique nano-scale microstructure of plant leaves under rainy conditions**

#### **Contents of this file**

Number of Figures: 13

Number of tables: 3

## **Supplementary Protocols**

### **Plant analysis**

(i) Roots, stems and leaves of peanut seedlings were carefully separated, and the plant morphology and fresh weight were determined.

(ii) The SPAD-502 chlorophyll meter (SPAD-502 plus, Konica, Minolta Inc, Japan) was used to obtain SPAD readings. Old leaves and young leaves were randomly selected separately for measurement in accordance with the previously established experimental protocol.

(iii) For this study, old leaves and young leaves were separately selected in a randomized manner based on previous experimental protocols, and the leaf photosynthesis parameters were assessed using a portable LI-6400 meter (LI-6400, LICOR Inc., Lincoln, NE, USA).

(iv) Tissue structure analysis: representative peanut young leaves were randomly selected as analysis objects in a treatment. SEM-EDS. Unwashed fresh leaf tissues measuring  $2 \times 2$  mm were sectioned and lyophilized using a freeze dryer (SCIENTZ-10N, Ningbo Xinzhi Biotechnology Co., Ltd., Ningbo, China), and then the samples were coated with gold particles for 5 seconds using a sputtering coater (E-1045, Hitachi, Tokyo, Japan). The microstructure and morphology of the stomata on the leaf surface were visualized through scanning electron microscopy (SEM, SU8082, Hitachi, Japan,

Japan), and the Fe -K $\alpha$  energy spectrum distribution pattern was provided by the energy dispersive spectroscopy (EDS).

(v) Nutrient analysis: The plant tissue (0.2 g) was completely digested using a mixture of HNO<sub>3</sub>-H<sub>2</sub>O<sub>2</sub> (5 mL and 2 mL, GR) in an automatic tissue digester (Auto Digiblock S60UP, LabTech, USA). After filtering the digest, the concentration of mineral nutrients in the digested solution was determined with an inductively coupled plasma spectrometer (ICP-OES, 5110 SVDV, Agilent, Santa Clara, CA, USA). The precision and accuracy of nutrient digestion and analysis methods were assessed through the analysis of certified standard substances (GBW10020, PR China) derived from citrus leaves.

(vi) Statistical analysis of the nanosheet structure and stomatal size in leaves: To prevent any potential deformations on the surface microstructure and stomatal shape of the leaves, we were drying leaves with CO<sub>2</sub> critical point method<sup>1</sup>. We collected 2×2 cm iron-deficient peanut and corn leaves, which were subsequently dried using the CO<sub>2</sub> critical point drying method. The dried leaf samples were then mounted on a sample platform and coated with palladium–gold using a Hitachi IB-5 ion plating instrument (Hitachi, Tokyo, Japan). Finally, the prepared samples were observed and photographed using scanning electron microscopy (SEM, SU8082, Hitachi, Japan, Japan). Then, the height/void size of the leaf nanosheets and stomatal shape of the

leaves was analyzed using the Nano Measurer 1.2 software. For detailed statistical mapping, please refer to the red line in Figure S1 and S2.

### **Evaluation of adhesion and anti-leaching of nano-iron particles on leaf surfaces**

The evaluation of adhesion and anti-leaching test is conducted in four stages, namely -A, B, C, D (Fig. S4): Stage A represents the period of plant culture prior to foliar application. During this stage, plants were subjected to iron starvation by growing them in an iron-free nutrient medium for 10 days. The background leaf iron content was determined based on the iron content of plant leaves during stage A; In stage B, 10 mL of nano-iron fertilizer prepared in 0.1% Tween 80 or 0.1% Tween 80 (for control) was uniformly sprayed onto the leaves of 6 peanut plants. During this stage, the iron content of plant leaves comprised both the background iron and the nano-iron particles taken up from the sprayed iron fertilizer; In stage C, a simulated rainfall of 100 mL water was applied to the leaves, 1 hour after foliar fertilizer application in stage B. The water spray resulted in partial loss of nano-iron fertilizers sprayed onto the leaves due to leaching; In the stage D, the leaves were separated and washed with 0.01 M HCl solution. During this stage, plant leaves exhibited inherent background iron content and a minimal uptake of nano-iron by the leaf tissue. The leaves from all four states were digested by  $\text{HNO}_3\text{-H}_2\text{O}_2$ , and the iron concentration was determined by ICP-OES. The effective

foliar application amount, the leaching amount and the effective adhesion amount of nano-iron were determined using the following formulas:

$$\text{The effective foliar application amount} = (B-A) \quad (\text{eq-S1})$$

$$\text{The leaching amount} = (B-C) \quad (\text{eq-S2})$$

$$\text{The effective adhesion amount} = (C-D) \quad (\text{eq-S3})$$

### **Contact angle model test**

The contact angle model refers to taking peanut leaves as solid and nano-iron fertilizer preparation as liquid. When the iron fertilizer solution is applied to the leaves, three interfacial tensions are formed: solid-gas, liquid-gas, and solid-liquid (Fig. S6). The surface free energies of the solid-gas, solid-liquid, and liquid-gas interfaces are denoted as  $\gamma_{sg}$ ,  $\gamma_{sl}$  and  $\gamma_{lg}$ , respectively. The contact angle ( $\theta$ ) refers to the angular measurement of the angle between the liquid–solid interface. The relationship between  $\gamma_{sg}$ ,  $\gamma_{sl}$ ,  $\gamma_{lg}$  and  $\theta$  complies with the wetting equation (Young equation shown in eq-S4)<sup>2,3</sup>. The contact angle  $\theta$  is directly correlated with the wetting degree of the solution. A smaller value of  $\theta$  indicates a higher degree of wetting, facilitating easier attachment to the leaves. This formula is shown in eq-S18.

$$\gamma_{sg} - \gamma_{sl} = \gamma_{lg} \cos \theta \quad \text{eq-S4}$$

The formula for the adhesion work ( $W_a$ ) is presented in eq-S5, which can be calculated by through the measurement of  $\gamma_{lg}$  (solution surface tension) and  $\text{COS}\theta$

(contact angle). Both  $\theta$  and  $\gamma_{lg}$  were measured using the contact angle measurement (PZ-200SD, Pinzhi Chuangsi Precision Instrument Co., Ltd, Beijing, China). It quantifies the adhesion ability of the solution on the solid surface This equation quantifies the adhesive ability of the nano-iron fertilizer solution to adhere to a leaf surface.

$$W_a = \gamma_{sg} + \gamma_{lg} - \gamma_{sl} = \gamma_{lg}(1 + \cos \theta) \quad \text{eq-S5}$$

### **Comparison analysis of the force/work of Fe<sub>3</sub>O<sub>4</sub> particles with different sizes on peanut and maize leaves**

i) When the size of Fe<sub>3</sub>O<sub>4</sub> particles exceeds 1000 nm (i.e., 10 $\mu$ m), they remain on top of the nanosheets of peanut/maize leaves and cannot fall into the void positions (Fig. 1.A/B).

As shown in Fig. 1.A/B, the Fe<sub>3</sub>O<sub>4</sub> particles were subjected to van der Waals force ( $F_{vdw}$ ), gravity (G), buoyancy force ( $F_b$ ), supporting force ( $F_s$ ), and friction force ( $F_f$ ) on the surface of the plant leaf, along with the impulsive force ( $F_i$ ) exerted by water droplets.

$F_{vdw}$  of Fe<sub>3</sub>O<sub>4</sub> particles on the plant leaf surface should be calculated using the following equation, eq-S6:

$$F_{vdw} = \frac{A}{6} \left[ \frac{rR}{Z_0(r+R)} + \frac{R}{(Z_0+r)^2} \right] \quad \text{eq-S6}$$

A indicates Hamaker constant ( $1 \times 10^{-20}$  J); r represents the height of nanosheets on the plant leaf surface (peanut:  $1.72 \times 10^{-7}$  m; maize:  $1.15 \times 10^{-7}$  m); R denotes 1/2 the size of  $\text{Fe}_3\text{O}_4$  particles (half of  $10 \mu\text{m}$ :  $0.5 \times 10^{-5}$  m);  $Z_0$  is the distance from the  $\text{Fe}_3\text{O}_4$  molecule to plant leaf surface (the estimated value presented here corresponds to the molecular radius:  $1 \times 10^{-10}$  m). Thus, the both  $F_{\text{vdw}}$  of  $\text{Fe}_3\text{O}_4$  particles on the peanut/maize leaf surface were calculated and shown in Table 1 and Table 2.

G of  $\text{Fe}_3\text{O}_4$  particles on the plant leaf surface should be calculated using the following equation, eq-S7:

$$G = \rho a^3 g \quad \text{eq-S7}$$

$\rho$  is material density ( $1.8 \times 10^3$  kg/m<sup>3</sup>); a denotes the size of  $\text{Fe}_3\text{O}_4$  particles ( $a = 1 \times 10^{-5}$  m); g is the gravity acceleration constant ( $g = 9.80$  m/s<sup>2</sup>). Thus, the G of  $\text{Fe}_3\text{O}_4$  particles was calculated to be  $1.77 \times 10^{-11}$  N.

$F_b$  of  $\text{Fe}_3\text{O}_4$  particles on the plant leaf surface should be calculated using the following equation, eq-S8:

$$F_b = \rho_{\text{H}_2\text{O}} a^3 g \quad \text{eq-S8}$$

$\rho_{\text{H}_2\text{O}}$  is water density ( $1.0 \times 10^3$  kg/m<sup>3</sup>); a denotes the size of  $\text{Fe}_3\text{O}_4$  particles ( $a = 1 \times 10^{-5}$  m); g is the gravity acceleration constant ( $g = 9.80$  m/s<sup>2</sup>). Thus, the  $F_b$  of  $\text{Fe}_3\text{O}_4$  particles was calculated to be  $0.98 \times 10^{-11}$  N.

$F_s$  can be calculated according to the following equation, eq-S9:

$$F_s = F_{vdw} + F_i \cos 45^\circ + G \cos 45^\circ - F_b \cos 45^\circ \quad \text{eq-S9}$$

The formula above can be used to calculate  $F_{vdw}$ ,  $G$ , and  $F_b$ .  $F_i$  is assumed to be a specific range value to simulate the impulse force exerted by the water droplets.

$F_f$  on the plan leaf surface can be calculated according to the following equation, eq-S10:

$$F_f = F_s \mu \quad \text{eq-S10}$$

The friction coefficient constant ( $\mu = 0.8$ ) of rubber-cast iron is referenced from ASTM International standard for ASTM G115<sup>4</sup>.

In order for  $\text{Fe}_3\text{O}_4$  particles to slide off the surface of a plant leaf, the following inequality conditions must be satisfied (eq-S11). Since  $F_{vdw}$  is much smaller than  $G$  and  $F_b$  and  $F_i$  (Table 1 and 2), it can be disregarded in the calculation process of eq-S11. According to  $\sin 45^\circ = \cos 45^\circ$ , eq-S12 can be further simplified from eq-S11.

$$F_f = F_s \mu = (F_{vdw} + F_i \cos 45^\circ + G \cos 45^\circ - F_b \cos 45^\circ) \mu \leq F_i \sin 45^\circ + G \sin 45^\circ - F_b \sin 45^\circ$$

eq-S11

$$\mu \leq 1 \quad \text{eq-S12}$$

Finally, the coefficient of friction ( $\mu$ ) for rubber-cast iron is 0.8, which aligns with eq-S12 and thus supports our results that  $\text{Fe}_3\text{O}_4$  particles (10  $\mu\text{m}$ ) exhibit easily slide off plant leaf surfaces.



ii) When the size of  $\text{Fe}_3\text{O}_4$  nanoparticles is below than 1000 nm and the height and distribution frequency (void size) of the peanut leaf nanosheets are large (Fig. 1.C/E), they experience a strong blocking effect from the nanosheets on peanut leaf, making it difficult for them to slide down.

As shown in Fig. 1.C, the  $\text{Fe}_3\text{O}_4$  nanoparticles were subjected to various forces, including van der Waals force ( $F_{\text{vdw}}$ ), gravity ( $G$ ), buoyancy force ( $F_b$ ), supporting force ( $F_s$ ), friction force ( $F_f$ ) and impulsive force ( $F_i$ ).

$F_{\text{vdw}}$  is also calculated using the eq-S6.  $A$  indicates Hamaker constant ( $1 \times 10^{-20}$  J);  $r$  represents the distance from the nanosheets molecule to  $\text{Fe}_3\text{O}_4$  particles surface (the estimated value presented here corresponds to the  $\text{Fe}_3\text{O}_4$  molecular radius:  $1 \times 10^{-10}$  m);  $R$  denotes 1/2 the size of  $\text{Fe}_3\text{O}_4$  nanoparticles ( $1/2 a = 5/10/25/50$  nm:  $5 \times 10^{-9}$  m,  $10 \times 10^{-9}$  m,  $25 \times 10^{-9}$  m,  $50 \times 10^{-9}$  m);  $Z_0$  is the distance from the  $\text{Fe}_3\text{O}_4$  molecule to plant leaf surface (the estimated value presented here corresponds to the molecular radius of leaf cuticle:  $1 \times 10^{-10}$  m). Thus, the  $F_{\text{vdw}}$  of  $\text{Fe}_3\text{O}_4$  nanoparticles on the peanut leaf surface was calculated and shown in Table 1.

$G$  can also be calculated using the eq-S7.  $\rho$  is  $\text{Fe}_3\text{O}_4$  nanoparticles density (the average density:  $4.95 \times 10^3$  kg/m<sup>3</sup>);  $a$  denotes the size of  $\text{Fe}_3\text{O}_4$  nanoparticles ( $a = 10/20/50/100$  nm:  $10 \times 10^{-9}$  m,  $20 \times 10^{-9}$  m,  $50 \times 10^{-9}$  m,  $100 \times 10^{-9}$  m);  $g$  is the gravity acceleration constant ( $g = 9.80$  m/s<sup>2</sup>). Thus, the  $G$  of  $\text{Fe}_3\text{O}_4$  nanoparticles was calculated and shown in Table 1.

Similarly,  $F_b$  is calculated using the eq-S8.  $\rho_{H_2O}$  is water density ( $1.0 \times 10^3 \text{ kg/m}^3$ );  $a$  denotes the size of  $Fe_3O_4$  nanoparticles ( $a=10/20/50/100 \text{ nm}:10 \times 10^{-9} \text{ m}, 20 \times 10^{-9} \text{ m}, 50 \times 10^{-9} \text{ m}, 100 \times 10^{-9} \text{ m}$ );  $g$  is the gravity acceleration constant ( $g = 9.80 \text{ m/s}^2$ ). Thus, the  $F_b$  of  $Fe_3O_4$  nanoparticles was calculated and shown in Table 1.

As the sliding direction of  $Fe_3O_4$  nanoparticles changes from inclined downward to inclined upward, its force analysis also changes with the slip direction. Therefore, the new calculation formula for  $F_s$  is as follows: eq-S13:

$$F_s = F_{vdw} + G \cos 45^\circ - F_b \cos 45^\circ \quad \text{eq-S13}$$

The new  $F_s$  can be calculated according to the eq-S13.  $F_{vdw}$ ,  $G$  and  $F_b$  can also be calculated, as shown in Table 1.

As the sliding direction of  $Fe_3O_4$  nanoparticles changes from a downward inclination to an upward inclination, its force analysis also changes with the slip direction. Therefore, the new inequality conditions must satisfy the following conditions as follows: eq-S14:

$$F_f = F_s \mu = (F_{vdw} + G \cos 45^\circ - F_b \cos 45^\circ) \mu \leq F_i - G \sin 45^\circ + F_b \sin 45^\circ$$

eq-S14

Since  $F_{vdw}$  is much larger than  $G$  and  $F_b$ ,  $G$  and  $F_b$  can be disregarded in the calculation process of eq-S14. According to  $G$  and  $F_b$  be disregarded, eq-S15 can be

further simplified from inequality eq-S14.  $F_i$  is assumed to be a specific range value to simulate the impulse force exerted by the water droplets.

$$F_{vdw}\mu \leq F_i \quad \text{eq-S15}$$

Ultimately, it can be inferred that  $F_{vdw}$  exerts the dominant force, and there is a direct correlation between the magnitude of this force and the reduced likelihood of slip for  $\text{Fe}_3\text{O}_4$  nanoparticles in water droplets.

As shown in Fig. 1.E, the  $\text{Fe}_3\text{O}_4$  nanoparticles primarily exert an anti-friction force as they slide upward along the nanosheet of leaf at a constant speed. The analysis of work is based on the above force analysis results ( $F_{vdw}$  is the dominant force). Therefore, the formula for calculating work is as follows (eq-S16):

$$W = F_f s = (F_{vdw} + G \cos 45^\circ - F_b \cos 45^\circ) \mu s \approx F_{vdw} \mu s \quad \text{eq-S16}$$

$s$  represents the length of the sliding distance of the  $\text{Fe}_3\text{O}_4$  nanoparticles along the nanosheets of plant leaf (the height of nanosheets on peanut leaf is 172 nm); the slip distance of the first iron nanoparticle =  $172 - 1/2 a$  nm and the slip distance of the second iron nanoparticle =  $172 - 3/2 a$  nm ( $a$  is the size of  $\text{Fe}_3\text{O}_4$  nanoparticles, Fig. 1.C);  $F_{vdw}$  is calculated using the above formula and  $\mu$  is 0.8. Finally,  $W$  can also be calculated and shown in Table 1.

iii) When the size of  $\text{Fe}_3\text{O}_4$  nanoparticles is less than 1000 nm and the height and distribution frequency of the leaf nanosheets are small (Fig. 1.D/F), they are caused by

excessive void size and small height of the nanosheets on maize leaf, resulting in reduced obstruction by the leaf nanosheets.

As shown in Fig. 1.D, the  $\text{Fe}_3\text{O}_4$  particles were also subjected to van der Waals force ( $F_{vdw}$ ), gravity ( $G$ ), buoyancy force ( $F_b$ ), supporting force ( $F_s$ ), and friction force ( $F_f$ ) on the surface of the plant leaf, along with the impulsive force ( $F_i$ ) exerted by water droplets.

$F_{vdw}$ ,  $G$  and  $F_b$  are calculated using the same formula as above for eq-S6, eq-S7 and eq-S8 respectively. Similar to the calculation in Fig. 1.B, these calculations of  $\text{Fe}_3\text{O}_4$  nanoparticles on the maize leaf surface were shown in Table 2.

As the sliding direction of  $\text{Fe}_3\text{O}_4$  nanoparticles is inclined downward, its force analysis also changes in comparison with Fig. 1.B. Therefore, the new calculation formula for  $F_s$  is as follows: eq-S17:

$$F_s = F_{vdw} + F_i \cos 45^\circ + G \cos 45^\circ - F_b \cos 45^\circ \quad \text{eq-S17}$$

The new  $F_s$  can be calculated according to the eq-S17.  $F_{vdw}$ ,  $G$  and  $F_b$  can also be calculated, as shown in Table 2. In order to satisfy the slip condition, the following inequality must be satisfied (eq-S18).

$$F_f = F_s \mu = (F_{vdw} + F_i \cos 45^\circ + G \cos 45^\circ - F_b \cos 45^\circ) \mu \leq F_i \sin 45^\circ - G \sin 45^\circ + F_b \sin 45^\circ$$

eq-S18

Since  $F_{vdw}$  is much larger than  $G$  and  $F_b$  (Table 2),  $G$  and  $F_b$  can be disregarded in the calculation process of eq-S16. According to  $\sin 45^\circ = \cos 45^\circ$ , eq-S19 can be further simplified from eq-S18.  $F_i \sin 45^\circ (1 - \mu)$  is a specific range value in the eq-S19.

$$F_{vdw}\mu \leq F_i \sin 45^\circ (1 - \mu) \quad \text{eq-S19}$$

As shown in Fig. 1.F, the  $\text{Fe}_3\text{O}_4$  nanoparticles primarily exert an anti-friction force as they slide upward along the nanosheet of leaf at a constant speed. The analysis of work is based on the above force analysis results ( $F_{vdw}$  is the dominant force). Therefore, the formula for calculating work is as follows (eq-S16):

$$W = F_f s = (F_{vdw} + F_i \cos 45^\circ + G \cos 45^\circ - F_b \cos 45^\circ) \mu s \approx F_{vdw} \mu s \quad \text{eq-S20}$$

$s$  represents the length of the sliding distance of the  $\text{Fe}_3\text{O}_4$  nanoparticles along the nanosheets of plant leaf (the height of nanosheets on maize leaf is 115 nm); the slip distance of the first iron nanoparticle =  $115 - 1/2 a$  nm ( $a$  is the size of  $\text{Fe}_3\text{O}_4$  nanoparticles, Fig. 1.C);  $F_{vdw}$  is calculated using the above formula and  $\mu$  is 0.8. Finally,  $W$  can also be calculated and shown in Table 2.

Ultimately, it can be inferred that  $F_{vdw}$  exerts the dominant force, and the larger the size within the range of 10-100 nm, the greater  $F_{vdw}$ ,  $F_f$  and  $W_{(n=1)}$ , making it less likely for particles to slip off from maize leaf surface.

## Supplementary Figures

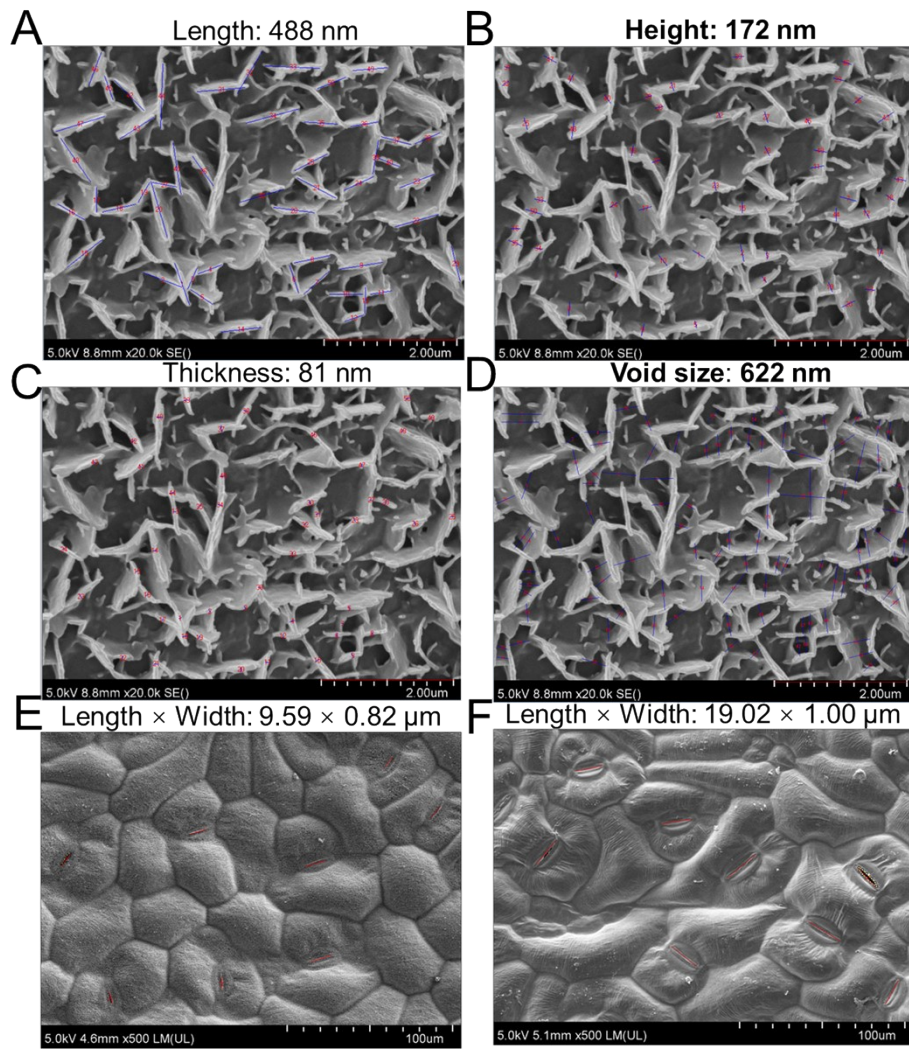


**Fig. S1.** Statistics of the nanosheets structure (A-D) and the stomata size on upper (E)/lower (F) epidermis in peanut leaves.

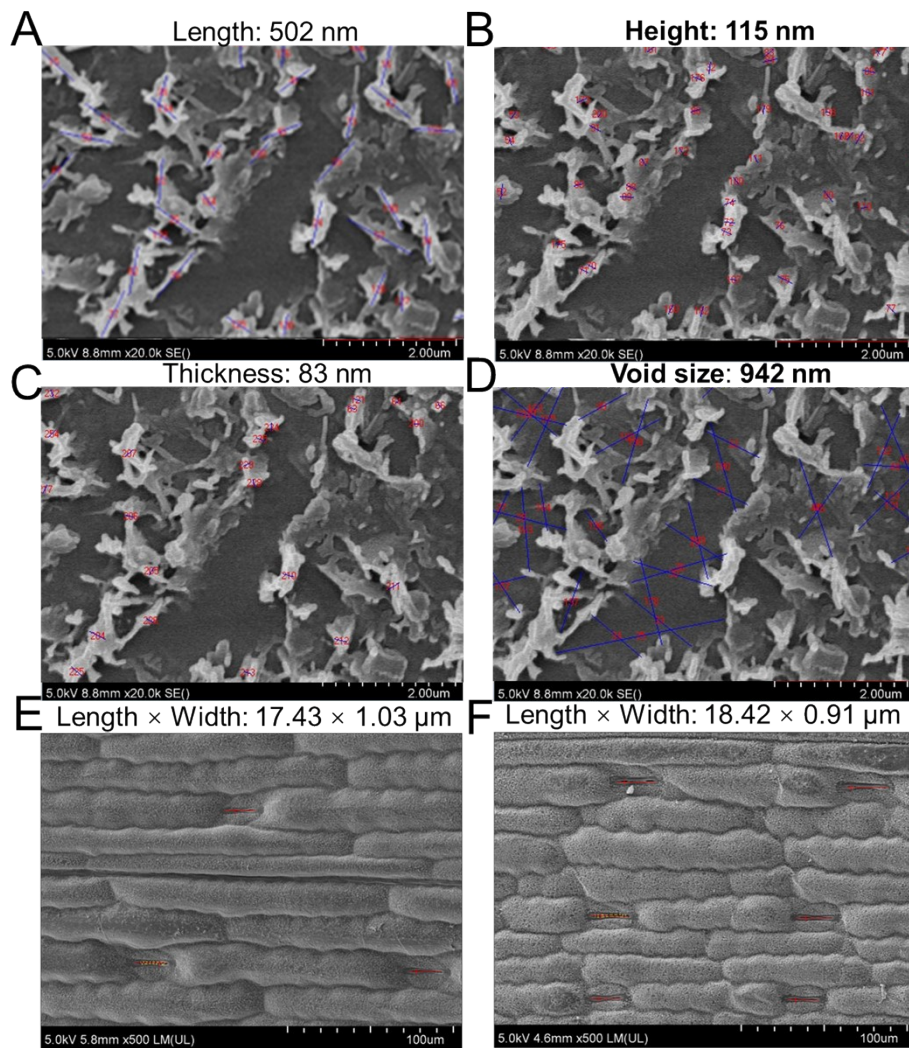


**Fig. S2.** Statistics of the nanosheets structure (A-D) and the stomata size on upper (E)/lower (F) epidermis in maize leaves.

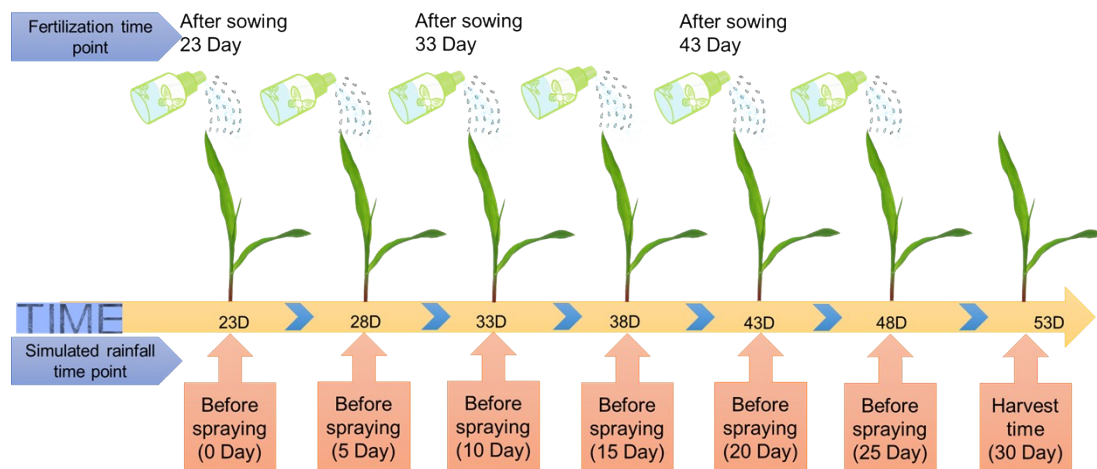


**Fig. S3.** Schematic diagram of the foliar fertilizations and simulated rainfall condition test. The fertilization time points were on days 23, 33, and 43 after sowing seeds. The simulated rainfall time points were on days 23, 28, 33, 38, 43 and 48 after sowing seeds. Adapted from Chen et al<sup>3</sup>.

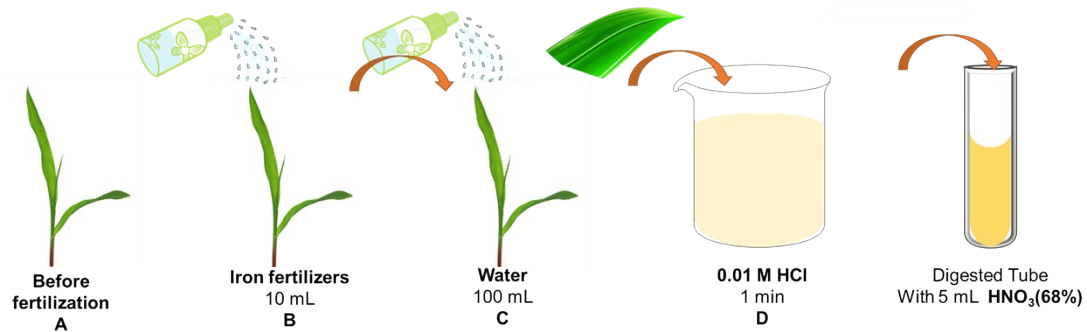


**Fig. S4.** A schematic diagram illustrating the leaf adhesion and anti-leaching test of nano-iron particles is presented, which consists of four distinct stages (A, B, C, D). The detailed description of these stages can be found in the methodology section above. Adapted from Chen et al<sup>3</sup>.

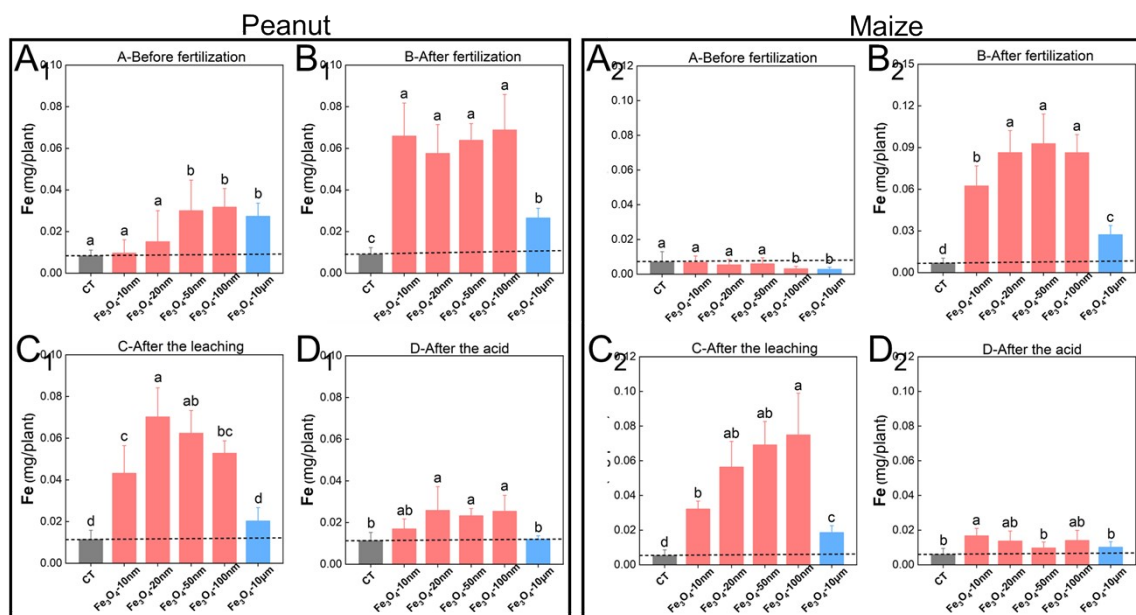




**Fig. S5.** The iron content of peanut (subscript 1) and maize (subscript 2) leaf: A- Before foliar application; B- Plants sprayed with 10 mL of nano-iron fertilizer; C- Plants sprayed with 100 mL of water to simulate rainfall after iron fertilizer application; D- Plants in treatment C after washing with 0.01M HCl. CT - 0.1% Tween 80 solution. Mean values  $\pm$  standard deviations ( $n = 6$ ), shown by the bar diagram, followed by different letters are significantly different according to Duncan's multiple range test ( $p < 0.05$ ).

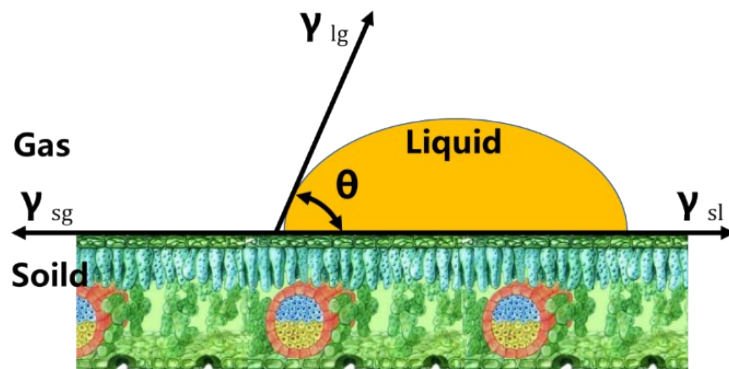


**Fig. S6.** Schematic diagram of the contact angle model. When the nano-iron fertilizers solution is sprayed on the leaves, three interfacial tensions such as solid-gas, liquid-gas and solid-liquid are formed. Adapted from Chen et al<sup>3</sup>.

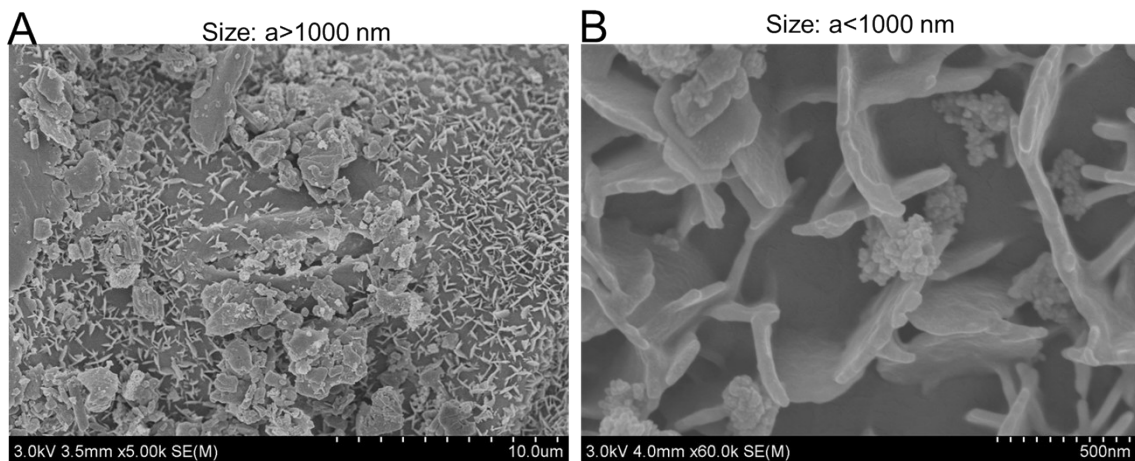


**Fig. S7.** A- When the size of  $\text{Fe}_3\text{O}_4$  particles exceeds 1000 nm (i.e.,  $10\mu\text{m}$ ), they stay on the nanosheets of plant leaves and cannot fall into the void positions; B- When the size of  $\text{Fe}_3\text{O}_4$  nanoparticles is less than 1000 nm (10-100 nm), they can be accommodated within the interstitial spaces of plant leaf nanosheets.

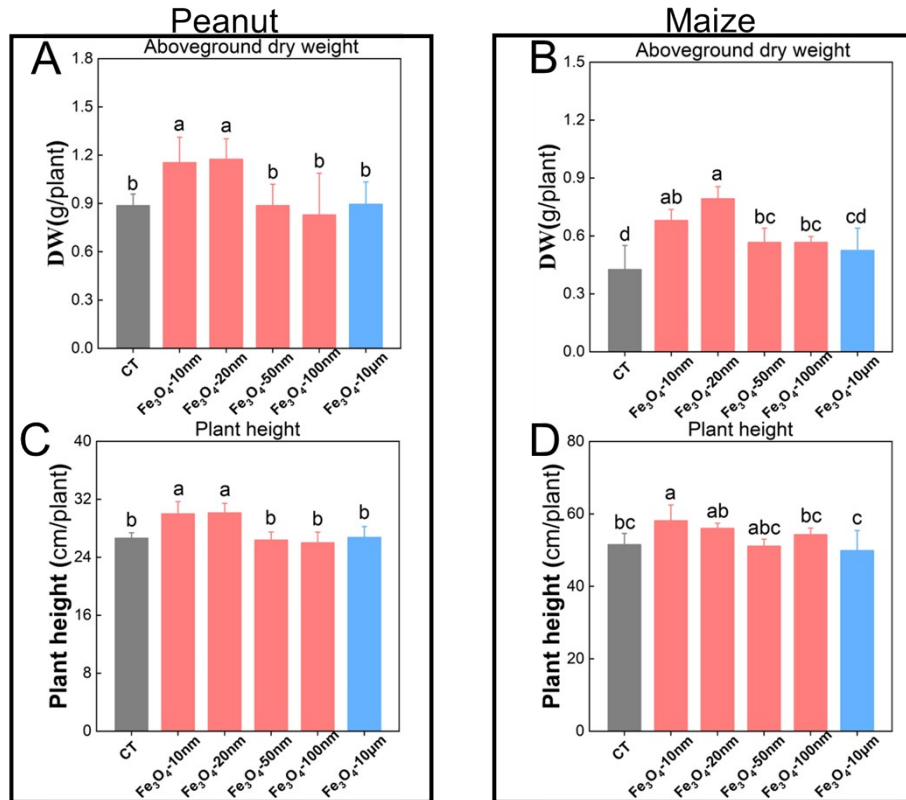


**Fig. S8.** Above-ground dry weight (A) and plant height (C) of peanut plants supplied with different nano-iron fertilizers by foliar application and grown at 53 days after sowing under non-rainfall conditions. Above-ground dry weight (B) and plant height (D) of maize plants supplied with different nano-iron fertilizers by foliar application and grown at 53 days after sowing under non-rainfall conditions. CT- 0.1% Tween 80 solution, DW- dry weight. Mean values  $\pm$  standard deviations ( $n = 4$ ), shown in the bar diagram, followed by different letters are significantly different according to Duncan's multiple range test ( $p < 0.05$ ).

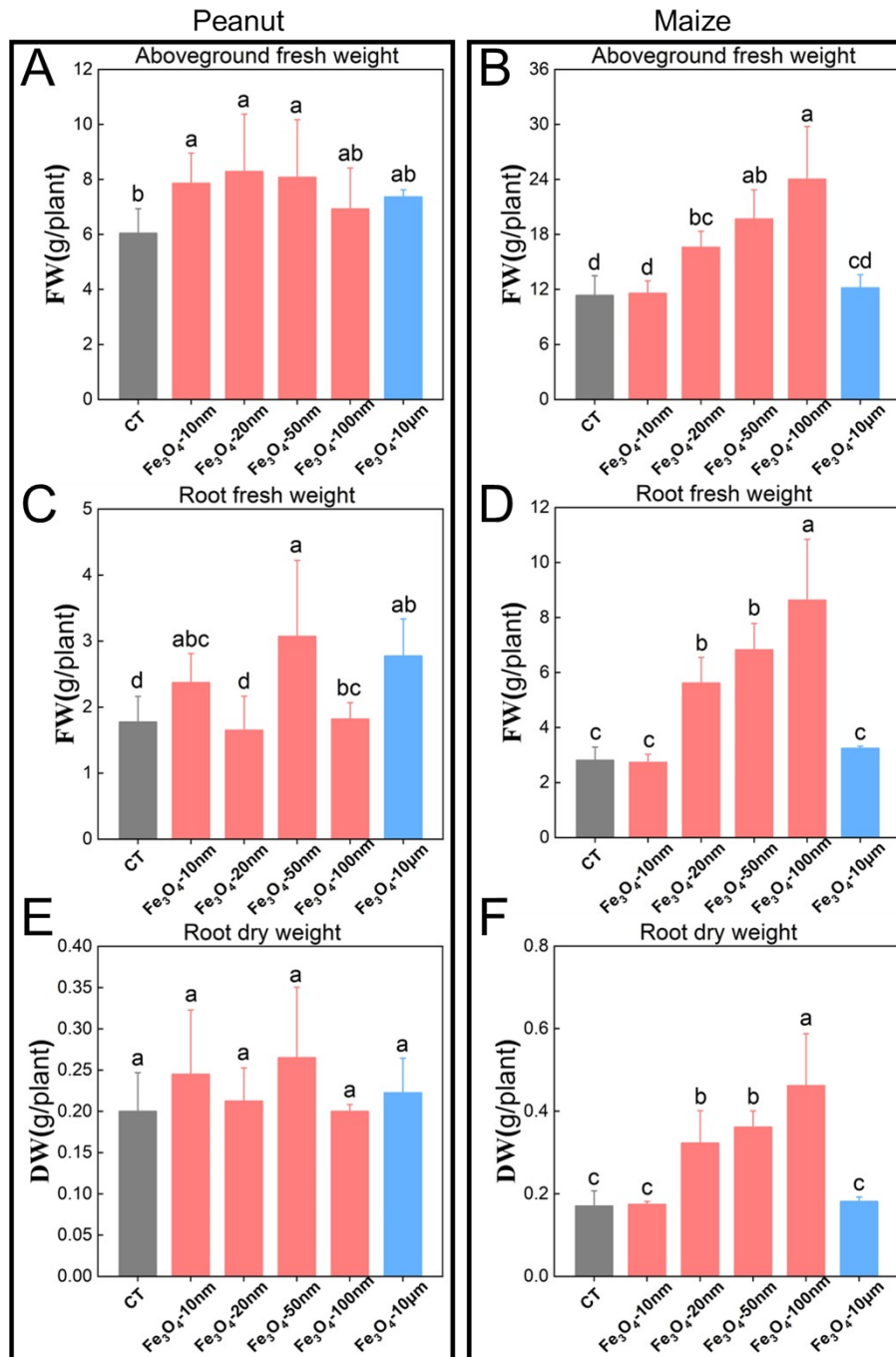


**Fig. S9.** Above-ground fresh weight (A), root fresh weight (C) and root dry weight (E) of peanut plants supplied with different nano-iron fertilizers by foliar application and grown at 53 days after sowing under simulated rainfall conditions. Above-ground fresh weight (B), root fresh weight (D) and root dry weight (F) of maize plants supplied with different nano-iron fertilizers by foliar application and grown at 53 days after sowing under simulated rainfall conditions. FW - fresh weight, DW - dry weight. CT - 0.1% Tween 80 solution. Mean values  $\pm$  standard deviation ( $n = 4$ ), shown by the bar diagram,

followed by different letters are significantly different according to Duncan's multiple range test ( $p < 0.05$ ).

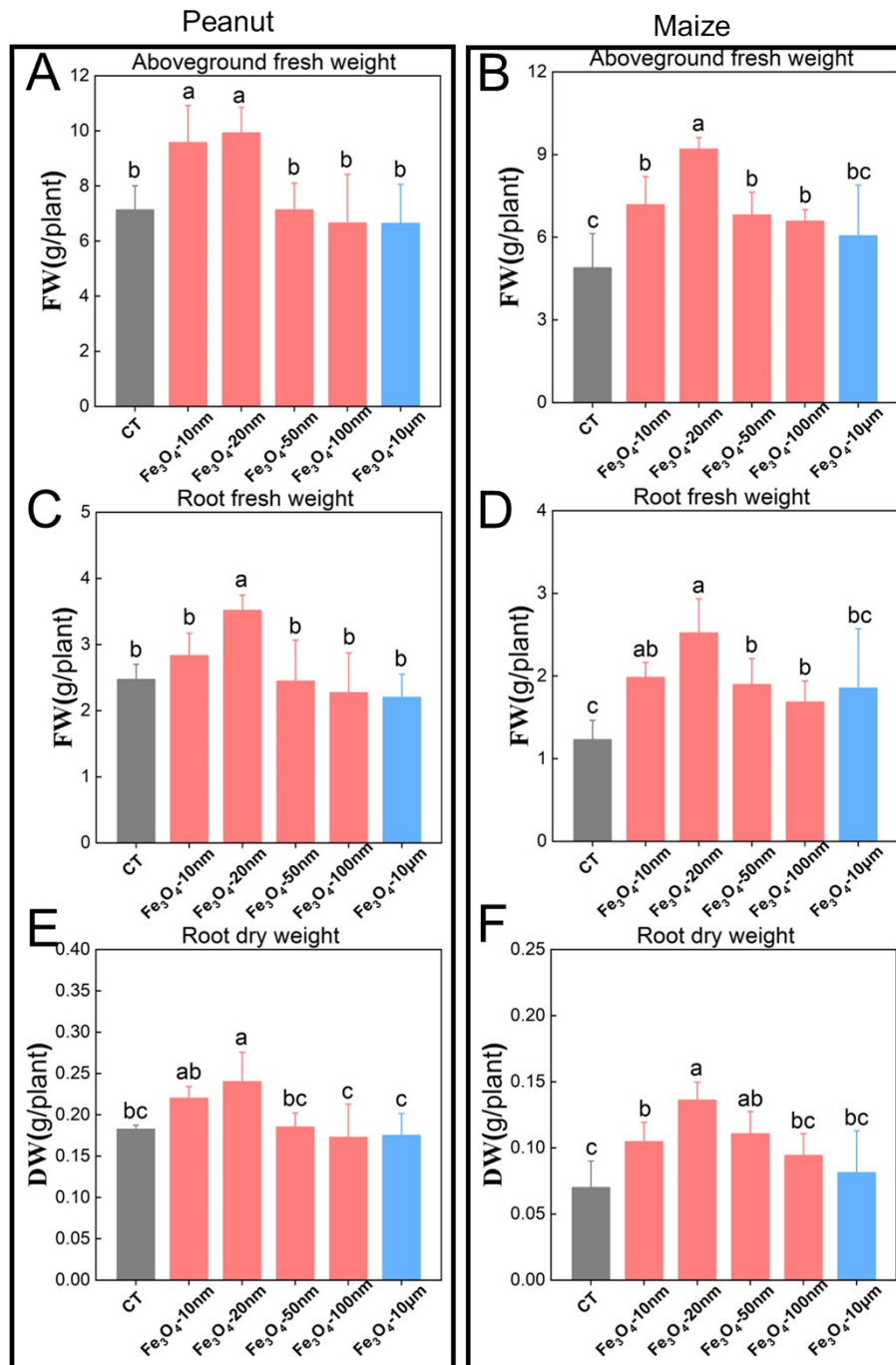


**Fig. S10.** Above-ground fresh weight (A), root fresh weight (C) and root dry weight (E) of peanut plants supplied with different nano-iron fertilizers by foliar application and grown at 53 days after sowing under non-rainfall conditions. Above-ground fresh

weight (B), root fresh weight (D) and root dry weight (F) of maize plants supplied with different nano-iron fertilizers by foliar application and grown at 53 days after sowing under non-rainfall conditions. FW - fresh weight, DW - dry weight. CT - 0.1% Tween 80 solution. Mean values $\pm$  standard deviation (n = 4), shown by the bar diagram, followed by different letters are significantly different according to Duncan's multiple range test (p < 0.05).

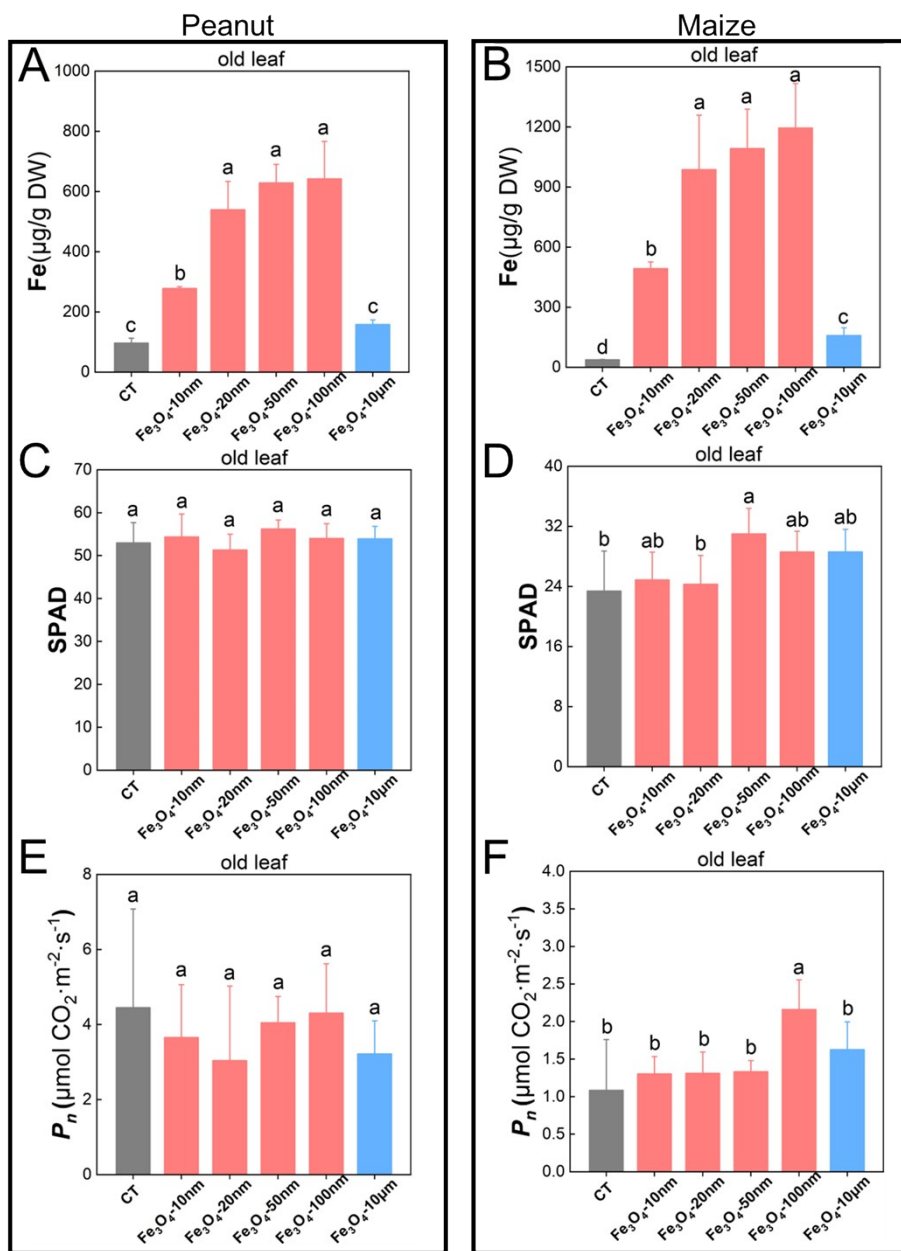


**Fig. S11.** Iron concentration (A), SPAD (C), and  $P_n$  (E) of old leaves of peanut supplied with different nano-iron fertilizers foliar application at 53 days after sowing under simulated rainfall conditions. Iron concentration (B), SPAD (D), and  $P_n$  (F) of old leaves of maize supplied with different nano-iron fertilizers foliar application at 53 days after sowing under simulated rainfall conditions. CT- 0.1% Tween 80 solution, DW- dry weight,  $P_n$ - net photosynthetic rate. Mean values  $\pm$  standard deviations (n = 6), shown in the bar diagram, followed by different letters are significantly different according to Duncan's multiple range test ( $p < 0.05$ ).

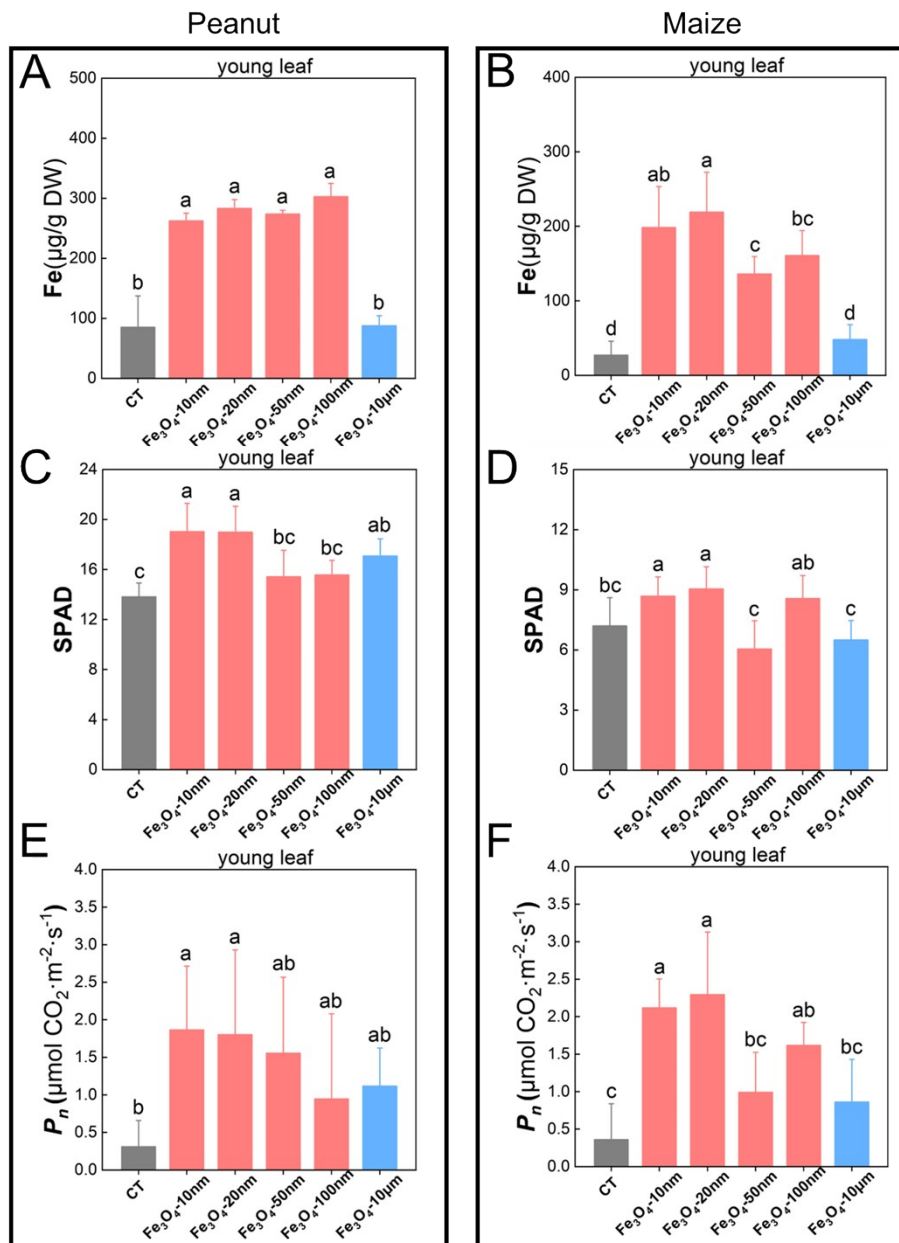


**Fig. S12.** Iron concentration (A), SPAD (C) and  $P_n$  (E) of young leaves of peanut supplied with different nano-iron fertilizers foliar application at 53 days after sowing under non-rainfall conditions. Iron concentration (B), SPAD (D) and  $P_n$  (F) of young leaves of maize supplied with different nano-iron fertilizers foliar application at 53 days after sowing under non-rainfall conditions. CT- 0.1% Tween 80 solution, DW- dry weight,  $P_n$ - net photosynthetic rate. Mean values  $\pm$  standard deviations ( $n = 6$ ), shown in the bar diagram, followed by different letters are significantly different according to Duncan's multiple range test ( $p < 0.05$ ).

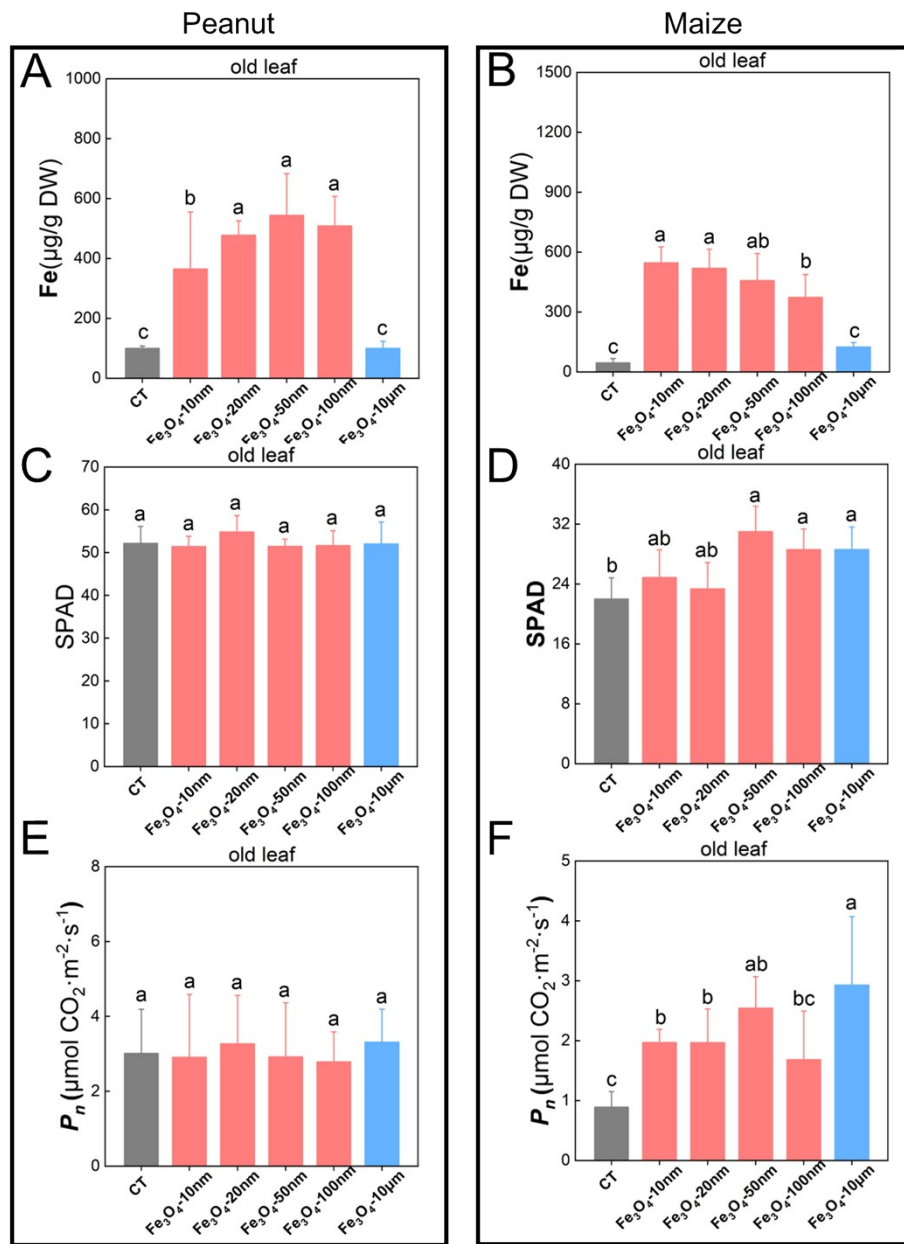


**Fig. S13.** Iron concentration (A), SPAD (C) and  $P_n$  (E) of old leaves of peanut supplied with different nano-iron fertilizers foliar application at 53 days after sowing under non-rainfall conditions. Iron concentration (B), SPAD (D) and  $P_n$  (F) of old leaves of maize supplied with different nano-iron fertilizers foliar application at 53 days after sowing under non-rainfall conditions. CT- 0.1% Tween 80 solution, DW- dry weight,  $P_n$ - net photosynthetic rate. Mean values  $\pm$  standard deviations (n = 6), shown in the bar



diagram, followed by different letters are significantly different according to Duncan's multiple range test ( $p < 0.05$ ).

### Supplementary table

**Table S1.** Statistics of the nanosheets structure and the stomata size on upper/lower epidermis in peanut and maize leaves.

Statistical parameters	Peanut	Maize
Height of nanosheets on plant leaves (nm)	172	115
Void size of nanosheets on plant leaves (nm)	622	942
Length of nanosheets on plant leaves (nm)	488	502
Thickness of nanosheets on plant leaves (nm)	81	83
Number of stomata on upper epidermis per $\text{mm}^2$ (No./ $\text{mm}^2$ )	178	67
Number of stomata on lower epidermis per $\text{mm}^2$ (No./ $\text{mm}^2$ )	161	133

Size of stomata on upper epidermis (Length/ $\mu\text{m}$ $\times$ Width/ $\mu\text{m}$ )	9.59 $\times$ 0.82	17.43 $\times$ 1.03
Size of stomata on lower epidermis ((Length/ $\mu\text{m}$ $\times$ Width/ $\mu\text{m}$ ))	19.02 $\times$ 1.00	18.42 $\times$ 0.91

---

**Table S2.** Modified Hoagland solution composition.

Macro-nutrients	Micro-nutrients
1 mM $\text{NH}_4\text{H}_2\text{PO}_4$	50 $\mu\text{M}$ Fe-EDTA $\cdot$ 3H <sub>2</sub> O
6 mM $\text{KNO}_3$	2 $\mu\text{M}$ $\text{ZnSO}_4\cdot 7\text{H}_2\text{O}$
1 mM $\text{MgSO}_4\cdot 7\text{H}_2\text{O}$	2 $\mu\text{M}$ $\text{MnSO}_4\cdot \text{H}_2\text{O}$
1 mM $\text{Ca}(\text{NO}_3)_2\cdot 4\text{H}_2\text{O}$	0.5 $\mu\text{M}$ $\text{H}_3\text{BO}_3$
	0.5 $\mu\text{M}$ $\text{Na}_2\text{MoO}_4\cdot 2\text{H}_2\text{O}$
	0.5 $\mu\text{M}$ $\text{CuSO}_4\cdot 5\text{H}_2\text{O}$
	0.25 $\mu\text{M}$ KCl
	0.005 $\mu\text{M}$ $\text{CoCl}_2\cdot 6\text{H}_2\text{O}$

---

**Table S3.** The hydrodynamic size and Zeta potential of different nano-iron fertilizers solution.

Iron fertilizer types	Hydrodynamic size (nm)	Zeta-potential (mV)
CT (0.1% Tween 80)	25±3d	-15.3±2.0a
Fe <sub>3</sub> O <sub>4</sub> -10 nm	379±11c	-14.7±2.4a
Fe <sub>3</sub> O <sub>4</sub> -20 nm	416±23c	-15.4±2.5a
Fe <sub>3</sub> O <sub>4</sub> -50 nm	1210±70b	-18.2±1.4a
Fe <sub>3</sub> O <sub>4</sub> -100 nm	1393±44b	-15.9±1.9a
Fe <sub>3</sub> O <sub>4</sub> -10 μm	2060±421a	-17.3±2.2a

Mean ± standard deviation (n = 3) shown in the bar diagram followed by different letters are significantly different according to Duncan's multiple range test ( $p < 0.05$ ).

## REFERENCES

- 1 B. Liu, C. Ou, S. Chen, Q. Cao, Z. Zhao, Z. Miao, X. Kong and F. Zhuang, Differentially expressed genes between carrot petaloid cytoplasmic male sterile and maintainer during floral development, *Sci. Rep.*, 2019, **9**, 17384.
- 2 W. Li, R. Fan, H. Zhou, Y. Zhu, X. Zheng, M. Tang, X. Wu, C. Yu and G. Wang, Improving the utilization rate of foliar nitrogen fertilizers by surface roughness engineering of silica spheres, *Envir. Sci. Nano*, 2020, **7**, 3526–3535.
- 3 L. Chen, Z. Hu, W. Chen, Z. Xu, C. Hao, P. Lakshmanan, D. Liu and X. Chen, Comparative study of the effectiveness of nano-sized iron-containing particles as a foliar top-dressing of peanut in rainy conditions, *Agr. Water Manage.*, 2023, **286**, 108392.
- 4 ASTM G115, 2008. Standard Guide for Measuring and Reporting Friction Coefficients, Annual Book of Standards, ASTM International, West Conshohocken, Pennsylvania, 492–503.